Fermi National Accelerator Laboratory

FERMILAB-Conf-90/260-E
[E-687]

Fermilab Experiment E-687: Recent Results on Charm *

The E-687 Collaboration

presented by

W. D. Shephard
University of Notre Dame
Notre Dame, Indiana 46556

December 1990

* Presented at the XXth International Symposium on Multiparticle Dynamics, Gut Holmecke, Germany, September 10-14, 1990.

Operated by Universities Research Association Inc. under contract with the United States Department of Energy

FERMILAB EXPERIMENT E687: RECENT RESULTS ON CHARM

P.L. Frabetti
Dip. di Fisica dell'Universita' and INFN - Bologna, I-40126 Bologna, Italy

C.W. Bogart, H.W.K. Cheung, P. Coteus, S. Culy, J.P. Cumalat, D. Kaplan
University of Colorado, Boulder, CO 80309, USA

J.N. Butler, F. Davenport, I. Gaines, P.H. Garbincius, S. Gourlay, D.J. Harding, P. Kasper, A. Kreymer, P. Lebrun, H. Mendez
Fermilab, Batavia, IL 60510, USA

S. Bianco, M. Enorini, F.L. Fabbri, A. Spallone, A. Zallo
Laboratori Nazionali di Frascati dell'INFN, I-00044 Frascati, Italy

R. Culbertson, M. Diesburg, G. Jaross, K. Lingel, P.D. Sheldon, J.R. Wilson, J. Wiss
University of Illinois at Urbana-Champaign, Urbana, IL 61801, USA

G. Alimonti, G. Bellini, M. Di Corato, M. Giammarchi, P. Inzani, S. Malvezzi, P.F. Manfredi, D. Menasce, L. Moroni, D. Pedrini, L. Perasso, A. Sala, S. Sala, D. Torretta, M. Vittone
Dip. di Fisica dell'Universita' and INFN - Milano, I-20133 Milan, Italy

D. Buchholz, C. Castoldi, B. Gobbi, S. Park, R. Yoshida
Northwestern University, Evanston, IL 60208, USA

J.M. Bishop, J.K. Busenitz, N.M. Cason, J.D. Cunningham, R.W. Gardner, C.J. Kennedy, E.J. Mannel, R.J. Mountain, D.L. Puseljic, R.C. Ruchti, W.D. Shephard, M.E. Zanabria
University of Notre Dame, Notre Dame, IN 46556, USA

S.P. Ratti, P. Vitulo
Dip. di Fisica Nucleare dell'Universita' and INFN - Pavia, I-27100 Pavia, Italy

A. Lopez
University of Puerto Rico at Mayaguez, Puerto Rico

Presented for Fermilab E687 Collaboration by W.D. Shephard

ABSTRACT

About 10^4 charm decays have been reconstructed from first-run data of Fermilab experiment E687 using the Fermilab Wide-Band Photon Spectrometer with the world's highest energy photon beam. Charm selection strategies and preliminary results are discussed. Lifetime values are (.50±.06±.03)ps for the D_s^+ and (.20±.03±.03)ps for the Λ_c^+. Preliminary D^+ and D^0 lifetimes are consistent with current world averages. Signals for charm baryon and Cabibbo-suppressed charm meson decays are shown. Preliminary branching ratios are: $B(D^0 \to \pi^+\pi^-\pi^+\pi^-)/B(D^0 \to K^-\pi^+\pi^+\pi^-) = .10\pm.02\pm.02$; $B(D^0 \to \overline{K^0}K^+K^-)/B(D^0 \to \overline{K^0}\pi^+\pi^-) = .20\pm.06$ (stat); $B(D^0 \to \overline{K^0}\phi)/B(D^0 \to \overline{K^0}\pi^+\pi^-) = .16\pm.06$(stat). Preliminary results are given on $D^{*\pm}$ and $D^{\pm,0}$ photoproduction for photon energies from 100 to 350 GeV.

1. Introduction and Spectrometer

Summarized here are preliminary results from the first run of Fermilab E687 in which about 45 million hadronic-event γBe triggers were recorded for γ energies up to about 350 GeV. Samples from the first run include about 10^1 reconstructed charm decays. Two complementary vertexing strategies were used for charm selection. More details are given in Ref. 1 and in Refs. 2 – 6, five recent Fermilab-FN notes by the E687 Collaboration. The second run of E687 will provide more than 5 times more data for future analysis.

The two magnet spectrometer includes a vertex detector and 5 multiwire proportional chambers of 4 planes each for charged-particle tracking. The vertex detector contains 4 sets of 3 views each of Si microstrip planes with pitch ranging from 25μm to 100μm for a total of about 8,000 channels. Its resolution, expressed as the predicted transverse error at the mean interaction point in the target for an infinite momentum track traversing the high-resolution region of the planes, is $\sigma_{X,Y} \approx 9\mu m$ corresponding to $\sigma_\tau \approx 0.03ps$. Neutral vees are reconstructed over a 10m decay length. Charged particles are identified by 3 multicell Čerenkov detectors with pion threshholds of 4.4, 6.7, and 17 Gev/c which provide identification of kaons from 17 to 44 GeV/c, protons from 17 to 44 GeV/c and 61 to 116 GeV/c, and "heavy" (K/p ambiguous) particles from 4.4 to 17 and 44 to 61 GeV/c. Electrons and photons are measured in 3 electromagnetic calorimeters, hadron energy is measured in 2 hadron calorimeters, and muons are identified by 2 sets of detectors. See Refs. 3 and 7 for more details.

The bremsstrahlung photon beam was produced by 350 GeV/c electrons with a 13% momentum spread striking a 27% radiator. Photon energy was measured by recoil electron detection. A Be target was used for most of the run. Data were taken with a trigger demanding at least two tracks in the spectrometer, both required to be outside the e^+e^-pair production region, and an energy deposit larger than a specified minimum (typically about 35 GeV) in the hadron calorimeter. Average photon energy for hadronic triggers was 221 GeV.

2. Vertexing and Charm Selection

Two basic approaches have been used in the selection of charm events:
– a stand-alone algorithm using only geometrical track information to construct the complete vertex topology of the event;
– a candidate-driven algorithm using the candidate vertex and momentum for a set of tracks consistent with a particular decay channel as a seed to find the primary vertex. Various requirements including net charge, Čerenkov identification, helicity cuts, minimum energy, etc. may be used in selecting the decay track combinations.
The first algorithm selects events on the basis of evidence for reconstructed secondary vertices; the second simply tests a hypothesis. As a result, the first method's efficiency tends to be smaller, especially at short lifetimes, but the final sample can be very clean. The second method's efficiency should depend less on proper time, but more

background at short lifetimes normally requires a cut on vertex separation L. Both techniques rely heavily on the resolution of the microstrip detector.

After event reconstruction, various subsamples (including charge conjugates) were selected by the methods described above. Results for $D^0 \to K^-\pi^+\pi^+\pi^-$ decays are shown. Figs. 1 a), b), c) show the effects of different cuts using the stand-alone vertexing method; figs. 1 d), e), f) show the D^0 signal from a candidate-driven vertex finder for several cuts on significance of vertex separation L/σ_L, where σ_L is the error in L. As expected, signal size decreases and signal-to-noise ratio improves as the L/σ_L cut increases. Larger signals may be obtained with the candidate-driven approach, but a cleaner sample may be obtained by the stand-alone approach without requiring a large vertex separation cut. Similar results for $D^0 \to K^-\pi^+$ and $D^+ \to K^-\pi^+\pi^+$ decays are shown in Ref. 4.

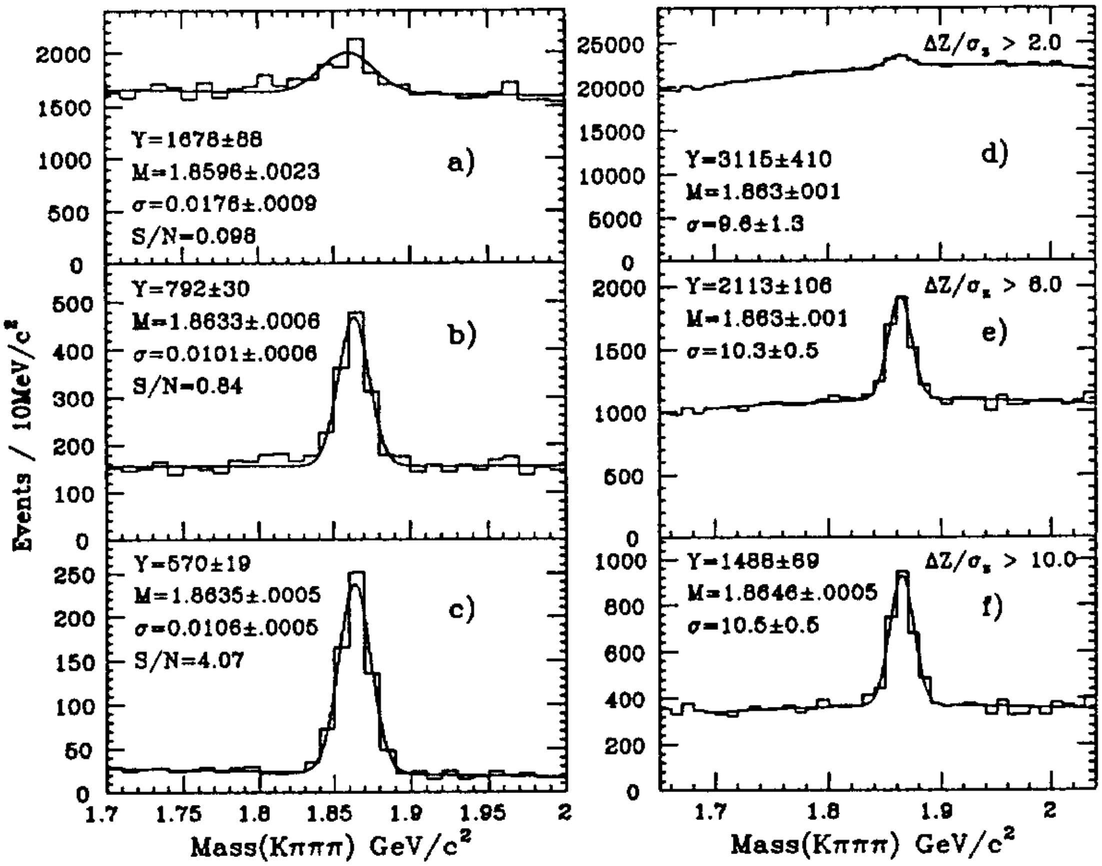

Fig. 1. $K^-\pi^+\pi^+\pi^-$ mass plots for event samples isolated with a), b), c) the stand-alone vertexing method: a) events with a reconstructed vertex of 4 linked tracks with zero net charge and compatible Čerenkov identification; b) events from plot a) with a reconstructed primary vertex in the target region; c) events from plot b) with D^0 candidate tracks pointing back to the primary vertex within $60\mu m$; and d), e), f) the candidate-driven vertexing method with different vertex separation cuts as indicated on the plots.

The success of the algorithms in selecting rarer decays is illustrated in Figs. 2 and 3. Fig. 2a) shows preliminary results obtained with the stand-alone algorithm for the difficult to isolate Cabibbo-suppressed $D^0 \rightarrow \pi^+\pi^-\pi^+\pi^-$ decay mode. Fig. 2b) shows the signal for the charmed baryon decay $\Lambda_c^+ \rightarrow pK^-\pi^+$ isolated with the candidate-driven approach. Fig. 3 shows samples (candidate-driven algorithm) of: a) and b) D_s^+ and D^+ decays to $\phi\pi^+$ from a subsample of the original data containing about 10^5 $\phi \rightarrow K^+K^-$ decays; c) $D^0 \rightarrow K_S^0K^+K^-$ decays obtained starting with a subsample containing about 10^6 $K_S^0 \rightarrow \pi^+\pi^-$ decays. E687 is fortunate to have two such highly successful complementary charm selection methods available.

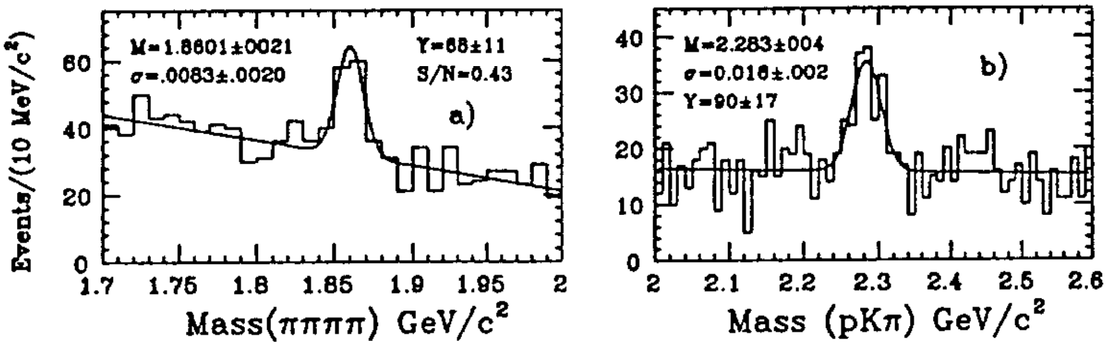

Fig. 2. Mass plots for a) $\pi^+\pi^-\pi^+\pi^-$ mass combinations from the stand-alone vertexing method, and b) $pK^-\pi^+$ mass combinations from the candidate-driven vertexing method.

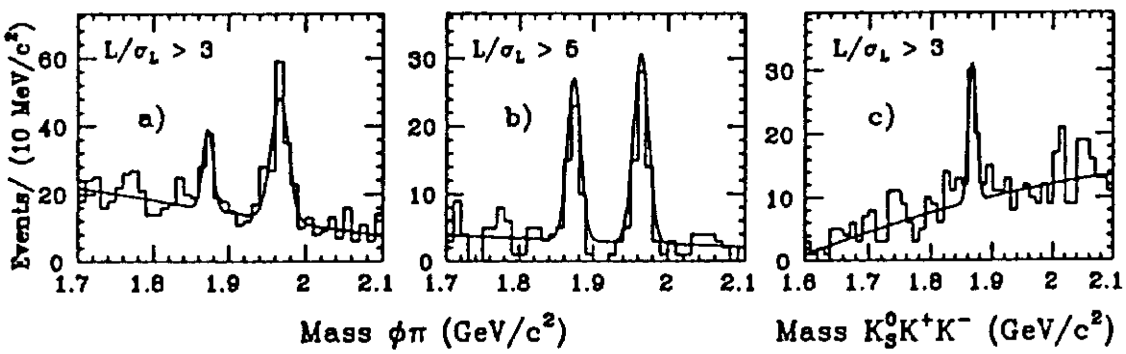

Fig. 3. Mass plots for rare charm decays isolated with the candidate-driven vertexing method: a) and b) $\phi\pi^+$ mass combinations for $L/\sigma_L > 3$ and $L/\sigma_L > 5$, respectively; c). $K_S^0K^+K^-$ combinations for $L/\sigma_L > 3$.

3. Lifetimes

Preliminary lifetime values for D^+ and D^0 mesons have been determined for samples from both techniques using binned maximum likelihood fits with a variety of background and efficiency parameterizations. More details are given in Ref. 4. Preliminary lifetimes of $(1.061\pm.039\pm.020)$ps, $(1.092^{+.056}_{-.048})$ps for $D^+\to K^-\pi^+\pi^+$ decays and $(.432\pm.016\pm.020)$ps, $(.461\pm.014)$ps for $D^0\to K^-\pi^+$ and $D^0\to K^-\pi^+\pi^+\pi^-$ decays have been found for samples from candidate-driven (stat. and syst. errors) and stand-alone algorithms (stat. errors only), respectively. These preliminary lifetimes are all in reasonable agreement with current world averages.[8]

Lifetimes for D_s^+ decaying to $\phi\pi^+$ and Λ_c^+ decaying to $pK^-\pi^+$ have also been determined using event by event maximum likelihood fits, with appropriate background and efficiency parametrizations, to proper time distributions for event samples obtained by the candidate-driven approach. Final lifetime values of $(0.50\pm0.06\pm0.03)$ps for the D_s^+ and $(0.20\pm0.03\pm0.03)$ps for the Λ_c^+ will be published soon.[9] In both cases the values are consistent with current world averages,[8] but continue the trend toward longer lifetimes seen in recent high-statistics results.

4. Branching Ratios

Much remains to be done to improve our knowledge of the many branching ratios and branching fractions for charm particles. E687 collaborators are engaged in studies of many charm decay channels, but final branching ratios require very careful determinations of such factors as Čerenkov identification efficiencies. Here we report preliminary branching ratios from work in progress.

Analysis of samples from a stand-alone algorithm of rare Cabibbo-suppressed $D^0\to\pi^+\pi^-\pi^+\pi^-$ decays (Fig. 2a) and of $D^0\to K^-\pi^+\pi^+\pi^-$ decays yields the preliminary value of $.091\pm.020$ for the ratio $B(D^0\to\pi^+\pi^-\pi^+\pi^-)/B(D^0\to K^-\pi^+\pi^+\pi^-)$. Independent analysis of samples from a candidate-driven algorithm yields a preliminary value of $.114\pm.030$ for the same ratio. Combining both estimates we obtain a preliminary estimate of $B(D^0\to\pi^+\pi^-\pi^+\pi^-)/B(D^0\to K^-\pi^+\pi^+\pi^-)=.10\pm.02\pm.02$ where the systematic error is estimated to be 2%. This may be compared with the current world average of about $.045\pm.018$ estimated from values in Ref. 8.

Preliminary results on $D^0\to K_S^0K^+K^-$ and $D^0\to K_S^0\,\pi^+\pi^-$ decays are also available. Of special interest is the decay $D^0\to\overline{K^0}\phi$ since it can, in principle, serve as a test for the presence of non-spectator decay processes.[10] Fig. 3c) shows a $K_S^0K^+K^-$ mass plot from a candidate-driven algorithm. Since $D^0\to K_S^0\,\pi^+\pi^-$ decays are more plentiful, tighter cuts can be put on that sample (not shown) which is used as the reference. Fitted signals are weighted as a function of D^0 momentum by the inverses of overall acceptance functions determined from Monte Carlo and other experimental studies.[6] The preliminary value (stat. errors only) for the inclusive branching ratio is: $B(D^0\to\overline{K^0}K^+K^-)/B(D^0\to\overline{K^0}\pi^+\pi^-)=.20\pm.06$. The world average calculated from branching fractions in Ref. 8 is about $.22\pm.05$.

The D^0 can be seen clearly in a two-dimensional scatter plot of K^+K^- mass as a function of $K_S^0K^+K^-$ mass for the $K_S^0K^+K^-$ sample and in the corresponding $K_S^0K^+K^-$ mass plot. A ϕ mass band and large ϕ peak are obvious at about 1.020 GeV/c^2 in the scatter plot and in the corresponding K^+K^-mass plot. There appears to be an enhancement where the bands overlap on the scatter plot (See Ref. 6.) To determine the fraction of $D^0 \rightarrow K_S^0K^+K^-$ decays via $D^0 \rightarrow K_S^0\ \phi$, we selected $K_S^0K^+K^-$ events with K^+K^-mass in a ϕ band, 1.010<M(K^+K^-)<1.030 GeV/c^2, and determined the D^0 signals in the resulting unweighted and weighted $K_S^0K^+K^-$ mass distributions; D^0 signals in sidebands, if present, are much smaller. The weighted D^0 signal corrected for $B(\phi \rightarrow K^+K^-)$ is used to estimate the branching ratio (statistical error only): B($D^0 \rightarrow \overline{K^0}\phi$)/B($D^0 \rightarrow \overline{K^0}\pi^+\pi^-$) = .16±.06 This preliminary value is consistent with the ARGUS result[11] of .155±.033. Fits to Dalitz plots will provide better estimates of $\overline{K^0}\phi$, $\overline{K^0}a_0(980)$ and non-resonant $\overline{K^0}K^+K^-$ contributions to the $D^0 \rightarrow \overline{K^0}K^+K^-$ channel and $K^{*-}\pi^+$, $\overline{K^0}\rho^0$, and non-resonant $\overline{K^0}\pi^+\pi^-$ contributions to the $D^0 \rightarrow \overline{K^0}\pi^+\pi^-$ channel.

5. Total Cross Sections and Production Mechanisms

Preliminary measurements have been made of photoproduction cross-sections for $D^{*\pm}$ and $D^{\pm}$ from two independent analyses of D^{*+} photoproduction. The first used the standard technique of cutting on the mass difference $\Delta M = M_{K\pi\pi} - M_{K\pi}$ to isolate the clean decay channel $D^{*+} \rightarrow D^0\pi^+$; $D^0 \rightarrow K^-\pi^+$.[12] This kinematic technique yielded a raw sample of 293±32 events from a restricted input data sample. An alternate technique using both the ΔM cut and finite lifetime cuts with a candidate-driven vertex algorithm provided raw samples of 1154±49 $D^{*+} \rightarrow D^0\pi^+$; $D^0 \rightarrow K^-\pi^+$ and $D^0 \rightarrow K^-\pi^+\pi^+\pi^-$ events, 1757±70 $D^+ \rightarrow K^-\pi^+\pi^+$ and 5379±248 $D^0 \rightarrow K^-\pi^+$ and $D^0 \rightarrow K^-\pi^+\pi^+\pi^-$ decays from a larger input data sample. The two D^{*+} analyses are complementary and provide a consistency check.

The fraction of D^0 from the D^{*+} decay chain is .237±.013, in reasonable agreement with a simple model which predicts .29±.02 with the assumption that D^*'s and D's are produced in proportion to the number of spin states available (3:1).[13] The D^* sample can be split according to charge as originating from D^{*+} or D^{*-} decays. The ratio of antiparticle to particle is split evenly within statistics (1.06 ± 0.08), providing no evidence for associated production of meson-baryon states at these energies.

The p_T^2 dependence of the cross section, corrected for limited x_F acceptance was calculated; the resultant differential cross sections for D^{*+} and D^+ are fitted by the empirical form $d\sigma/dp_T^2 \propto \exp(-bp_T^2 + cp_T^4)$, with b = 1.14±.23 (.92±.05) and c = .098±.045 (.036±.007) for the $D^{*+}(D^+)$. The average p_T^2 for $D^{*+}(D^+)$ derived from the differential cross-section data is $\langle p_T^2 \rangle$ = 1.33±.68 (1.26±.19) GeV^2/c^2, consistent with the values observed[13] by E691.

Total open charm photoproduction cross sections have been obtained from luminosity, spectrometer acceptance, and reconstruction and analysis efficiencies using samples from both analyses for photon energy ranges from 100 to 350 GeV . The observed energy dependence is reasonably consistent with results at lower energies. Predictions of the photon-gluon fusion model for m_c=1.5 GeV using a naive gluon distribution and a higher order perturbative QCD radiative correction agree well, within the theoretical uncertainties of the QCD parameters, with the experimental data. More details of the analyses and model calculations are given in Ref. 2.

6. Acknowledgements

We wish to acknowledge the assistance of the staffs of Fermilab, INFN of Italy and the physics departments of the University of Colorado, University of Illinois, Northwestern University, and Notre Dame University. This research was supported in part by the National Science Foundation, the U.S. Department of Energy, the Italian Istituto Nazionale di Fisica Nucleare and Ministero della Universita' e della Ricerca Scientifica.

7. References

1. P.L. Frabetti et al., "Recent Results On Charm From Fermilab Experiment E687", to be published in *Proceedings of the 25th International Conference on High Energy Physics, Singapore (August, 1990).*
2. "Photoproduction of D Mesons", FERMILAB-FN-90/555, submitted to Singapore Conference by D. Buchholz.
3. "Description of the E687 Spectrometer", FERMILAB-FN-90/553, submitted to Singapore Conference by S. Gourlay.
4. "D^+ , D^0 Signals and Lifetimes in E687 Photoproduction Experiment at Fermilab", FERMILAB-FN-90/556, submitted to Singapore Conference by L. Moroni.
5. "Measurement of the J/Ψ Elastic Photoproduction from 100 GeV to 400 GeV in the experiment E687 at Fermilab", FERMILAB-FN-90/554, submitted to Singapore Conference by S.P. Ratti.
6. "Some Lifetimes and Branching Ratios for Charmed Hadrons Produced in the Fermilab Wide-Band Photon Beam", FERMILAB-FN-90/557, submitted to Singapore Conference by W. D. Shephard.
7. P.L. Frabetti et al., "Description and Performance of the E687 Spectrometer", to be submitted *to Nuclear Instruments and Methods.*
8. Particle Data Group, *Phys. Lett.* **B239** (1990).
9. P.L. Frabetti et al., "Measurement of the $D_s^+$and Λ_c^+ Lifetimes", accepted for Publication in *Phys. Lett* B (1990); also FERMILAB-Pub-90/158-E [E687].
10. I.I. Bigi and M. Fukugita, *Phys. Lett.* **B91**, 121 (1980).
11. H. Albrecht et al., *Phys. Lett.* **B158**, 525 (1985).
12. S. Park, Ph.D. Thesis, Northwestern University, unpublished (1990).
13. J.C. Anjos et al., *Phys. Rev. Lett.* **62** (1989) 513.